Colloid Polym Sci 277:483–487 (1999)


SHORT COMMUNICATION

T. Okubo
K. Kobayashi
A. Kuno
A. Tsuchida

# Kinetic study of the formation reaction of colloidal silica spheres by transmitted-light-intensity and dynamic light-scattering measurements

Received: 10 November 1998
Accepted in revised form: 12 January 1999

T. Okubo (✉) · K. Kobayashi
A. Kuno · A. Tsuchida
Department of Applied Chemistry
Gifu University
Gifu 501-1193, Japan
e-mail: okubotsu@apchem.gifu-u.ac.jp
Fax: +81-580-2932628

**Abstract** Kinetic analyses of the formation reaction of colloidal silica spheres which are synthesized from ethyl silicate (EtSi), ammonia and a trace of water in ethanol are made by the transmitted-light-intensity and dynamic light-scattering methods. Sphere size versus time profiles from the two methods agree well especially at the beginning of the reaction. The polymerization starts after a certain induction time ($t_i$) ranging from several tens of seconds to several minutes. $t_i$ increases as the concentrations of $NH_3$, EtSi and/or $H_2O$ decrease. The apparent rates of the reaction, $v'$ are estimated from the reciprocal periods between the intersections of the linear line with the initial and final horizontal lines in the cube root of the absorbance versus time plots. Log $v'$ increases linearly with slopes of 1, 2 and 0.5 as the logarithms of the concentrations of EtSi, $NH_3$ and/or $H_2O$ increase, respectively. These results are consistent with the assumption proposed earlier that the polymerization mechanism of the formation of the small preliminary particles is followed by their coalescence to form large silica spheres.

**Key words** Colloidal silica formation – Kinetics of polymerization – Transmitted-light intensity – Dynamic light scattering

## Introduction

In this work kinetic properties of the formation reactions of colloidal silica spheres in gravity have been studied in order to compare them with those in microgravity. The specific gravity of the colloidal silica spheres about 2.2 is very high compared with that of the solvent, ethanol in this work (0.82). Thus, this reaction is very convenient for studying microgravity effects. The microgravity experiments using aircraft will be followed in this series of studies. There have been significant developments in techniques for colloidal silica synthesis and these have been accompanied by recent advances in the sol–gel method in the field of fine ceramics [1–3]. The reaction system for colloidal silica synthesis was first reported by Stober et al. in 1968, and has been studied further by several researchers [4–18]. The polymerization reaction is composed of the hydrolysis of silicate, Eq. (1), and then the dehydration accompanied with the three-dimensional cross-linking, Eq. (2).

$$Si(OC_2H_5)_4 + 4\,H_2O \rightarrow Si(OH)_4 + 4\,C_2H_5OH \quad (1)$$

$$\equiv Si{-}OH + HO{-}Si\equiv \rightarrow \equiv Si{-}O{-}Si\equiv + H_2O \quad (2)$$

According to Shimohira and coworkers [7, 19] the primary small particles are formed first during an induction period, $t_i$, at the beginning of the reaction. Their critical size was estimated to be 10–20 nm [7]. The growth process with the coalescence of the primary particles then follows, and the final silica spheres are formed.

Shimohira et al. proposed that the sixth-order of sphere size increases linearly with reaction time, Eq. (3),

$$d^6 \propto t. \quad (3)$$

It should be recalled that Lifshitz–Slyozov–Wagner theory supports the second- and third-order relations for the surface reaction-controlled and diffusion-controlled mechanisms, respectively [20]. Furthermore, fourth- and fifth-order relations have been proposed for the surface diffusion and the diffusion accompanied with dislocation in the cases of ceramics and metal formations, respectively [20, 21]. Several experiments, however, have supported the sixth- or seventh-order relations [22–24], and theoretical explanations for the relationship have not been successful. Recently, a small-angle X-ray scattering study [18] revealed that after an induction period the first particles to appear in the solution have a radius of gyration of about 10 nm and are mass fractals characterized by their polymeric open structure. This report does not support the growth model proposed by Shimohira et al., for example.

## Experimental

### Materials

Tetraethyl orthosilicate (EtSi) was guaranteed grade and was purchased from Wako Pure Chemicals (Osaka). Ethanol (EtOH, 99.5%) and ammonia (25%) were the most purified grade reagents commercially available and were obtained from Wako Chemicals. The water used for the sample preparation was purified by a Milli-Q reagent grade system (Milli-RO5 Plus and Milli-Q Plus, Millipore, Bedford, Mass.).

### Transmitted-light-intensity and dynamic light-scattering measurements

Transmitted-light intensities (TLI) and the absorbances at 600 nm were taken on a spectrophotometer (Beckmann, DU650). The diameters of the colloidal silica spheres formed were determined using a dynamic light-scattering (DLS) spectrophotometer (DLS-7000, Otsuka Electronics, Osaka). The reaction was started by adding the EtOH solution of $NH_3$ and $H_2O$ to the EtOH solution of EtSi in the optical cell. Time-resolved TLI and DLS measurements were also made on a fast-scanning spectrophotometer (FTLI, MCPD-2000, Otsuka) and a fast-scanning dynamic light-scattering spectrophotometer (FDLS, ALV-5000, ALV Langen, Germany), respectively. These fast-scanning instruments were originally made for microgravity experiments and were connected with a stopped-flow-type mixer (MX-10, Otsuka) and a flow-type observation cell made of quartz glass. The reaction was started by mixing the same amounts of the EtOH solutions of $NH_3$ and EtSi, and they were introduced into the flow cell within a few milliseconds.

## Results and discussion

### Phase diagram of the reaction mixtures

Figure 1 shows the phase diagram of the reaction mixtures, where aqueous $NH_3$ was replaced with $H_2O$. The upper part of the diagram containing open circles shows the region where the mixtures are homogeneous and transparent. The crosses in the lower part of the diagram, on the other hand, show the heterogeneous mixtures where they are not mixed homogeneously and they are slightly turbid. Here, replacement of aqueous $NH_3$ with $H_2O$ is believed not to influence the phase diagram so much. Most of the kinetic measurements were made for the homogeneous mixtures.

### Sphere size versus time profiles, induction periods and apparent reaction rates from TLI measurements

Typical examples of absorbance ($A$) versus time profiles for the formation reaction of colloidal silica spheres when the concentration of $NH_3$ varies from 0.84 wt% to 8.4 wt% are shown in Fig. 2. Clearly, the absorbance

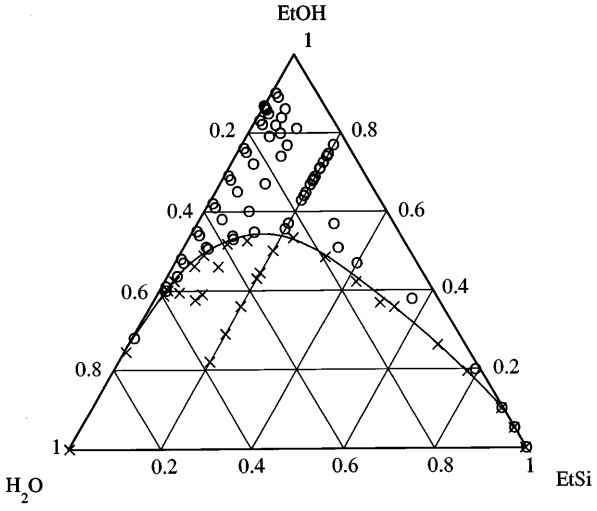


**Fig. 1** Phase diagram of tetraethyl orthosilicate (*EtSi*) + ethanol (*EtOH*) + $H_2O$ mixtures in volume fraction at 25 °C

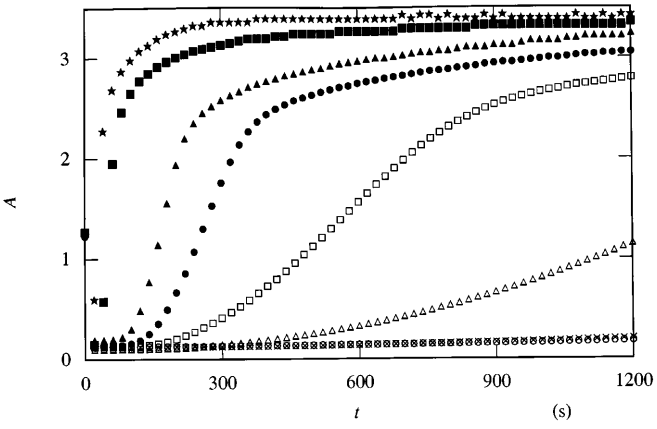


**Fig. 2** Plots of absorbance ($A$) against time ($t$) for colloidal silica formation at 25 °C. [EtSi] = 20 vol%, [$H_2O$] = 2 vol%, at 600 nm, ○: [$NH_3$] = 0.84 wt%, ×: 1 wt%, △: 1.4 wt%, □: 1.8 wt%, ●: 2.3 wt%, ▲: 2.8 wt%, ■: 5.6 wt%, ★: 8.4 wt%

increased after a certain induction time, $t_{i,}$ and $t_i$ decreased as the $NH_3$ concentration increased. Furthermore, the reaction was enhanced substantially when the $NH_3$ concentration increased. Plots of absorbance against time when the concentration of EtSi varies from 0.1 to 50 vol% are shown in Fig. 3. The $t_i$ values decreased and the reaction proceeded faster as the EtSi concentration increased. It should be noted here that when the concentrations of the reactants were high as described above part of the reaction mixtures were not homogeneous. The plots of absorbance versus $H_2O$ concentration have been studied, though the graph showing this has been omitted. $t_i$ decreased and the absorbance increased fast, respectively, as the concentration of $H_2O$ increased from 0 to 8 vol%.

The $t_i$ values were determined from the plots of absorbance versus reactant concentration. As is clear in Figs. 4 and 5, the $t_i$ values observed are always longer than 10 s and decrease as the EtSi concentration and/or the $NH_3$ concentration increase, respectively. It is interesting to note that the $t_i$ values showed a minimum around 10 wt% $NH_3$ and did not decrease any more even when the concentration of $NH_3$ increased further (see Fig. 5).

The absorbance value from the TLI measurements consists of the solvent absorption ($A_o$), the particle absorption ($A_p$), and the light-scattering at $\theta$ (scattering angle) = 0 ($A_s$), i.e., Eq. (4) [4].

$$A = A_o + A_p - A_s \tag{4}$$

The $A_p$ term arising from the colloidal spheres formed in the reaction should increase linearly with increasing volume of the sphere as,

$$A_p \propto Nd^3 \ , \tag{5}$$

where $N$ is the number of spheres formed in the reaction and $d$ is the diameter of the spheres. It should be noted here that Eq. (4) holds only if absorption dominates the scattering. When this is the case, $A_p \propto Nd^6$ holds. The light-scattering term, $A_s$, is further approximated by Eq. (6),

$$A_s \propto \ln(I_p \times I_i + I_m) \tag{6}$$

where $I_p$ is the intensity of the scattered light from the particle-form factor at $\theta = 0$. $I_i$ is the intensity of scattered light contributed from the interference factor at $\theta = 0$. This term reflects the particle distribution in the reaction mixtures. $I_m$ is the multiple-scattering term and is important especially in the final stage of the polymerization reaction, where large-sized colloidal spheres grow. The diameter, $d$, and the reaction rate, $v$, given by the growth rate of the sphere size are,

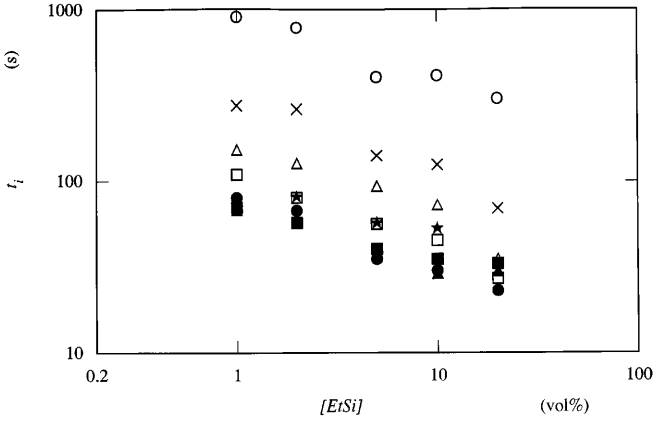


**Fig. 4** Induction periods in the course of colloidal silica formation at 25 °C. $[H_2O] = 2$ vol%, ○: $[NH_3] = 1.75$ wt%, ×: 3.5 wt%, △: 5.25 wt%, □: 7 wt%, ●: 8.75 wt%, ▲: 10.5 wt%, ■: 12.25 wt%, ★: 14 wt%

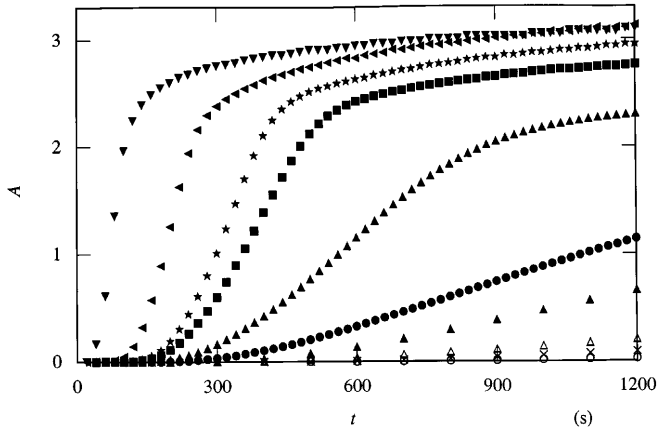


**Fig. 3** Plots of the $A$ against $t$ for colloidal silica formation at 25 °C. $[NH_3] = 2.8$ wt%, $[H_2O] = 2$ vol%, at 600 nm, ○: [EtSi] = 0.1 vol%, ×: 0.2 vol%, △: 0.3 vol%, □: 0.5 vol%, ●: 1 vol%, ▲: 2 vol%, ■: 5 vol%, ★: 10 vol%, ◀: 20 vol%, ▼: 50 vol%

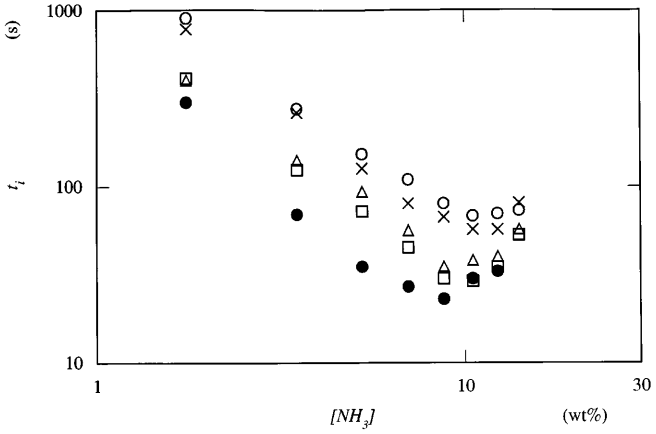


**Fig. 5** Induction periods in the course of colloidal silica formation at 25 °C. $[H_2O] = 2$ vol%, ○: [EtSi] = 1 vol%, ×: 2 vol%, △: 5 vol%, □: 10 vol%, ●: 20 vol%

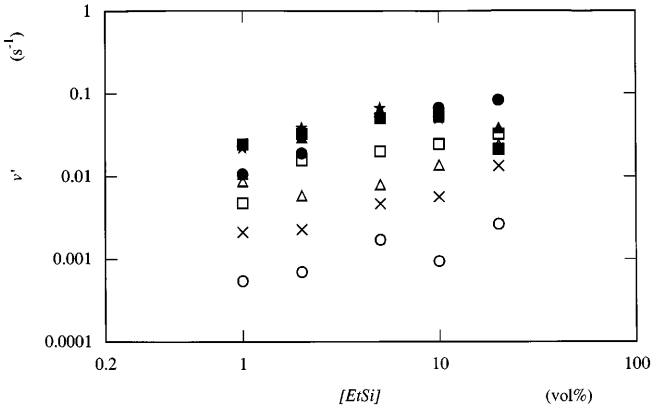


**Fig. 6** Apparent rates in the course of colloidal silica formation at 25 °C. $[H_2O]=2$ vol%, ○: $[NH_3]=1.75$ wt%, ×: 3.5 wt%, △: 5.25 wt%, □: 7 wt%, ●: 8.75 wt%, ▲: 10.5 wt%, ■: 12.25 wt%, ★: 14 wt%

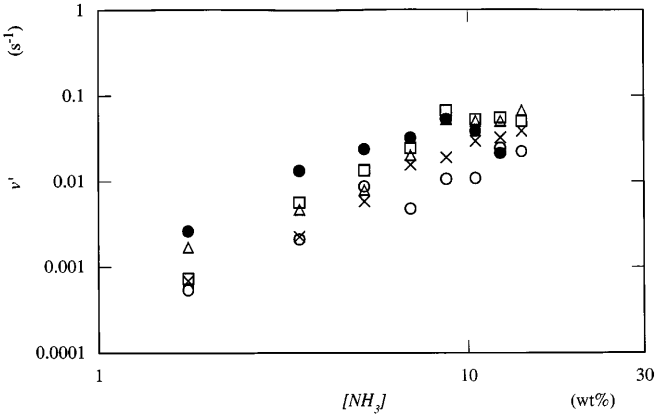


**Fig. 7** Apparent rates in the course of colloidal silica formation at 25 °C. $[H_2O]=2$ vol%, ○: [EtSi] = 1 vol%, ×: 2 vol%, △: 5 vol%, □: 10 vol%, ●: 20 vol%

therefore, approximated very roughly by Eqs. (7) and (8), respectively, especially at the beginning of the polymerization reaction. However, several reports have clarified that in the early stages of the particle-formation process the particle number does not always remain constant. Furthermore, the internal microstructure of the spheres becomes denser, and the absorption should change with time. Thus, we should note that the analyses using Eqs. (7) and (8) are not so reliable and contain rather large errors.

$$d \propto A_p^{1/3} \propto A^{1/3} \tag{7}$$

$$v = \mathrm{d}(d)/\mathrm{d}t \propto \mathrm{d}(A^{1/3})/\mathrm{d}t \tag{8}$$

The apparent reaction rates, $v'$ were determined from the reciprocal periods where the initial linear lines in the plots of cube root of the absorbance against time cross the initial ($t=0$) and final saturated horizontal lines, respectively. It should be noted that $v'$ denotes the reaction rate $v$ divided by the final size of colloidal spheres formed. The $v'$ values were obtained with high accuracy though the graphs showing the $A^{1/3}$ versus $t$ plots have been omitted. The logarithms of the $v'$ values increased with slopes of 1, 2 and 0.5 as ln [EtSi], ln[$NH_3$] and/or ln[$H_2O$] increased, respectively (e.g., see Figs. 6, 7).

## Sphere size versus time profiles from DLS measurements and their comparison with those from the TLI method

The plots of the diameters from the DLS and the cube root of the absorbance from the TLI methods are shown in Fig. 8. It should be mentioned here again that the $d$ values from the TLI method are not so reliable, since the method contains several assumptions as already described. On the other hand, the DLS technique gave the size data directly; however, it did not afford reliable data

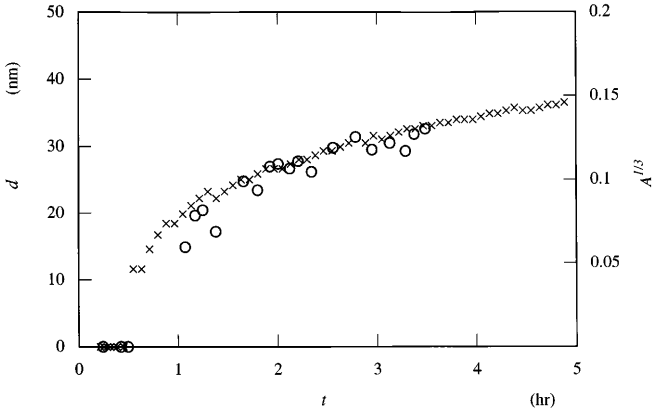


**Fig. 8** Diameters from dynamic light-scattering (○) and the cube root of the absorbance from transmitted-light-intensity (×) measurements in the course of colloidal silica formation at 25 °C. [EtSi] = 1.4 vol%, $[NH_3]=0.6$ wt%, $[H_2O]=0$ vol%

on diameters smaller than 10 nm. Our experiments clearly show that the sizes of the preliminary small silica particles are smaller than 10–20 nm and are too small to be determined precisely by DLS techniques. Discussion on the reaction order of colloidal silica formation was quite difficult in this work.

In conclusion, both the induction times and the reaction rates were evaluated by the TLS and DLS methods. Our results support the fact that the colloidal silica formation reaction is one of the most convenient polymerization systems for investigating the microgravity effect.

**Acknowledgements** Financial and technical support from the Frontier Research Project of the Japan Space Utilization Promotion Center and the National Space Development Agency of Japan (NASDA) are greatly acknowledged. T.O. thanks Sei Hachisu for his interest and valuable comments on this work.

## References


1. Iler RK (1979) The chemistry of silica. Wiley, New York
2. Klein LC (ed) (1988) Sol–gel technology for thin films, fibers, preforms, electronics and specialty shapes. Noyes, Park Ridge, N.J.
3. Bergna HE (1994) The colloid chemistry of silica. American Chemical Society, Washington, DC
4. Stober W, Fink A, Bohn E (1968) J Colloid Interface Sci 26:62
5. van Helden AK, Vrij A (1980) J Colloid Interface Sci 78:312
6. Kops-Werkhoven MM, Fijnant HM (1980) In: Degiorgio V, Corti M, Giglio M (eds) Light-scattering in liquids and macromolecular solutions. Plenum, New York, p 81
7. Shimohira T, Ishijima J (1981) Jpn J Chem Soc 1503
8. Okubo T (1988) J Chem Phys 88:6581
9. Matsoukas T, Gulari E (1988) J Colloid Interface Sci 124:252
10. Matsoukas T, Gulari E (1989) J Colloid Interface Sci 132:13
11. Bogush GH, Zukoski IV CF (1991) J Colloid Interface Sci 142:1
12. Bogush GH, Zukoski IV CF (1991) J Colloid Interface Sci 142:19
13. van Blaaderen A, van Geest J, Vrij A (1992) J Colloid Interface Sci 154:481
14. van Blaaderen A, Kentgens APM (1992) J Non-Cryst Solids 149:161
15. Okubo T (1992) Ber Bunsenges Phys Chem 96:61
16. Giesche H (1994) J Eur Ceram Soc 14:189
17. Lee K, Look JL, Harris MT, Mc Cormick AV (1997) J Colloid Interface Sci 194:78
18. Boukari H, Lin JS, Harris MT (1997) J Colloid Interface Sci 194:311
19. Shimohira T, Komuro N (1976) Powder Metall 23:137
20. Shewnon PG (1964) Trans Metall Soc AIME 230:1134
21. Nichols FA (1966) J Appl Phys 37:4599
22. Heg AW, Livey DT (1966) Trans Br Ceram Soc 65:626
23. Kotera Y, Saito T, Terada M (1963) Bull Chem Soc Jpn 36:2195
24. Aihara K, Chaklader ACD (1975) Acta Metall 23:855